A Solar Drying System for Vegetable Crops Design, Construction, and Performance Evaluation

Neeraj Kumar Singh Patel
Department of mechanical engineering
Rabindranath Tagore University
Raisen Bhopal (M.P.)
neerajksp1296@gmail.com

Rohit Pathak
Assistant Professor in the department of mechanical engineering institute of science & technology rabindranath tagore university Raisen Bhopal (M.P.)
rirt.rohitpathak86@gmail.com

Vinay Yadav
Professor in the department of mechanical engineering institute of science & technology rabindranath tagore university Raisen Bhopal (M.P.)
vinayyadav1211@yahoo.com

Abstract- ***The design, construction, and performance of a mixed-mode solar dryer for vegetable crops are presented in this study. A mixed-mode solar dryer takes advantage of both direct solar radiation from the sun and heat ducted from the solar collector inlet, which is directly connected to the dryer. Such dryers have been proven to outperform passive solar dryers, as demonstrated by drying kinetics in this study. Tomatoes were dried in a mixed-mode dryer in the drying room. The maximum dryer temperature was 43.0 degrees Fahrenheit, while the lowest relative humidity was 32.8 percent. These circumstances are only fair for drying tomatoes because they lengthen the drying period. Poor insolation and substantial heat losses on the designated drying days had a significant impact on the system's performance. During the chosen drying days, a drying rate of 2.92 units/day was obtained based on drying kinetics. The drier can dry 2kg of tomatoes in three days at this rate. Within 45 hours of drying time, the drier can reduce the moisture content of 1kg of tomatoes from 96 percent to 13 percent. The dryer has a capacity of 1kg of items per tray. The temperature distribution in the drying chamber is modelled using a basic 2D transient heat transfer model. Material selection, insolation, and intake temperature all play a part in the solar dryer's performance, according to the findings.***

Keywords- mixed-mode solar dryer, relative humidity, Tomatoes, Thermal-Convection, vegetable crops,

I. INTRODUCTION

Solar drying systems for agricultural products have been shown to be cost-effective, dependable, and ecologically friendly in the preservation of fruits, vegetables, and other crops [1]. These solar dryers provide another option for safely processing vegetables and fruits in accordance with industry standards. Minimal maintenance expenses, no fuel costs, time savings, occupying less space, improved product quality, environmental protection, and control of essential air condition are just a few of the benefits of these solar dryers [2].In many regions where food processing technologies such as indirect solar drying are required, there is a scarcity of reliable information about efficient solar dryers. Indirect drying with forced convection air flow is one of the finest alternatives for reducing the risk of spoiling during drying and ensuring high-quality product manufacturing [3]. Despite the fact that the solar air collector is a critical component of the sun drying system, it has received little attention during dryer design. The solar dryer's performance is influenced by a number of factors, including the weather, collection orientation, cover material thickness, wind speed, collector length and depth, and absorber material [4].

Drying products with renewable energy sources, such as solar energy, is more environmentally friendly and has a lower impact [5, 6]. Solar dryers of various varieties have been invented, built, and tested in various tropical and subtropical climates.Fruits and vegetables are essential components of the human diet. Post-harvest losses of around 40% [7] have become a major issue, and due to a lack of suitable storage techniques, there is only a limited ability to preserve and store commodities for off-season use.

A. Scope

This project is confined to the design, manufacture, and testing of a mixed-mode solar dryer utilising tomatoes as the test crop. The experiment and simulation are used to investigate the performance of the dryer under particular conditions, according to our novel design and analysis of the drying process. Materials will be chosen based on material attributes that are significant to the solar dryer's performance throughout the material selection phase. We shall, however, concentrate on tomato drying. In this mixed-mode condition, the drying rates of the tomatoes will also be investigated.

II. METHODOLOGY

B. Design of the dryer

The three principal sections of the dryer were developed as follows

C. Solar collector:

The solar collector consists of the following components: glazing (perspex glass), absorber plate, black-painted pebble rocks, insulation, inlet, collector side, solar PV system, fans, and stand. The glazing (perspex glass), absorber plate, black-painted pebble rocks, insulation, inlet, collector side, solar PV system, fans, and stand make up the solar collector**.**

Published By:
International Journal of Engineering Research in Current Trends

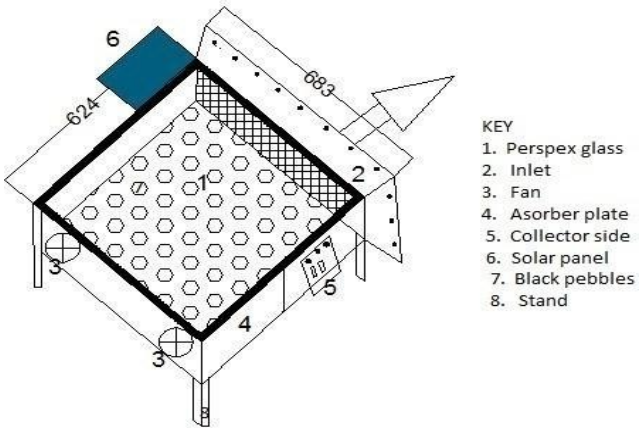

Figure 3.1: The solar collector

D. Drying chamber:

The drying chamber consists of the chimney, the glass roof, the glass walls, the trays, and the glass floor. Below is the engineering drawing showing the three parts (i.e. the trays, the solar collector, and the drying chamber) in the coupled form. The tray: The drying tray is made up of a wire mesh and wood. The wood is fastened to the mesh to form a rectangular shape when viewed from the top as shown below.

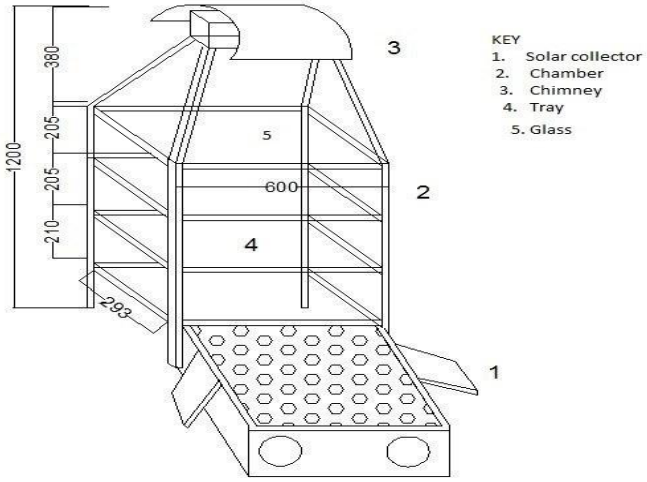

Figure 3.2: Design of the mixed-mode solar dryer

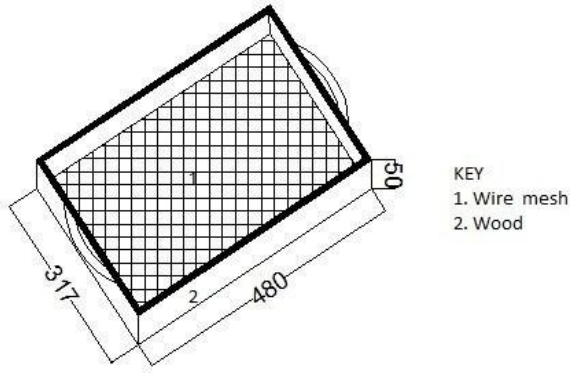

Figure 3.3: Design of the tray

E. Experimental Procedure for Performance Evaluation

The experiment comprised of three parts:

1. Temperature measurements: Starting on June 14, 2021, the hourly temperature variation of the primary components of the solar dryer was observed in the presence of the product (tomatoes). The technique was repeated two more times on June 15th and 16th, 2021. This was accomplished with the help of a digital thermometer that monitors temperatures between 25 and 50 degrees Fahrenheit.
2. Relative humidity measurements: The hourly relative humidity variation of the major parts of the solar dryer in the presence of the product (tomatoes) was calculated using the August-Roche-Magnus (ARM) approximation, also known as the Magnus formula, on each of the chosen days in the presence of the product (tomatoes). The following is a rough estimate based on the ARM approximation:

   Relative humidity (RH) is given by:

   $$RH \approx \frac{exp(17.625Td/243.04+Td)}{exp(17.625T/243.04+T)} \times_{100\%}$$

   RH = Relative humidity, *Td* = dew point, *T* = [-20^oC, 50°C]. *T* is the temperature range within which the formula holds.

   The use of a hygrometer is the most accurate means of determining relative humidity. We had to improvise because the instrument wasn't available, so we used the ARM approach.
3. Moisture content/Weight loss/Mass loss measurements: Using a weighing balance, the product's hourly weight loss or mass loss was assessed and translated to percentage moisture content loss.

F. Modeling Performance of the Dryer

The collector efficiency, overall heat loss coefficient, and heat removal factor are the three most critical metrics for a solar collector. The following is the theoretical background for these parameters [12]:

1. Flat-plate air heater collector efficiency:

At any given time, the collector efficiency is a dimensionless metric that measures the ratio of heat production from the inlet to heat input from the solar collector surface. It is a time-varying parameter that is affected by insolation, collector area, and the amount of heat extracted per unit time from hot air. This is how it's written:

$$\eta_c = \frac{\dot{Q}}{A_c S}$$

, where $Q = m_a c_p (T_{ab} - T_a)$

Where $\dot{m}_a$ = mass flow rate of heated air, cp = air specific heat capacity at constant pressure, and Tab denotes the temperature of the absorber or plate, whereas Ta denotes the temperature of heated air or the entrance. c is the collector efficiency, ac is the collector area, Q is the heat extracted from the heater per unit time, and Q is the heat extracted from the heater per unit time.

1. Coefficient of overall heat loss:

The total heat loss from the solar collector is measured in three areas: the top, the edge, and the rear contact or insulation. This is how it's written:

$U_l = U_t + U_b + U_e$,

$U_e \propto \frac{1}{A_c}, U_b \propto \frac{1}{\delta_b}, U_t \propto \frac{1}{R_t}$

where U_l = overall heat loss coefficient, U_t = overall top loss coefficient, U_b = overall back contact loss coefficient, U_e = overall edge loss coefficient, R_t = thermal resistance through the collector top, δ_b = thickness of back contact or insulation, and A_c = area of the collector.

2. Heat removal factor:

The heat removal factor is a dimensionless parameter that determines how easily heat may be extracted from the air heater's duct (inlet). This is how it's written: $F = \frac{Q}{[S-U_l(T_a-T_{am})]}$

where F is the heat removal factor, S is the insolation, Tam is the ambient temperature, Ta is the heated air temperature or inlet temperature, Ul is the overall heat loss coefficient, and Q is the heat extracted from the heater per unit time.

Table 3.4: Performance optimization of major dryer parts

Material	General properties	Thermal properties	Optical properties	Mechanical properties
Perspex Glass (glazing)	Density: 1.16 to 1.22kg/m^3 Price: cheap	low thermal conductivity	Transparent	Fracture toughness: 0.7 to 1.6MPa
Silica Glass (chamber)	Density: 2.15 to 2.2 × $10^3 kg/m^3$ Price: cheap	low thermal conductivity	Transparent	Fracture toughness: 0.6 to 0.8MPa
Aluminum (Chimney and chamber)	Density: 2.5 to 2.9 × $10^3 kg/m^3$ Price: Costly	high thermal conductivity	Opaque	Ductile
Mild steel (Absorber plate)	Density: 7.8 to 7.9 × $10^3 kg/m^3$ Price: cheap	high thermal conductivity	Opaque	Ductile

3. Heat Distribution in the Drying Chamber

Using the heat equation, we investigated a simplified model of two-dimensional transien heat transfer in the drying chamber. When some beginning circumstances are specified, the goal of this model is to obtain the transient temperature distribution in the drying chamber.

The temperature distribution is 2D in this case, i.e. T = T. (x,y,t) This model was built on the following assumptions:

1. The sun shines through the front wall, illuminating the chamber.

2. The inlet temperature is the same as the dryer's base temperature.

3. The exit temperature is the same as the dryer's top temperature.

4. The back wall's temperature is lower than the front wall's.

5. The dryer's length and breadth are the same.

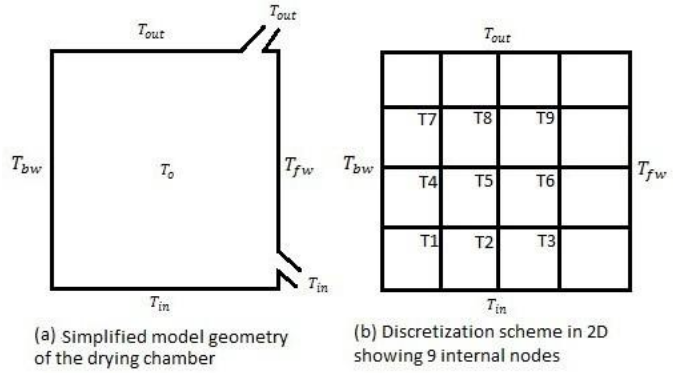

Figure 3.8: 2D model geometry of the transient heat distribution in the drying chamber

Tfw = temperature of the drying chamber's front wall in, Tbw = temperature of the drying chamber's rear wall in, Tout = outlet temperature, Tin = inlet temperature in, and To = beginning temperature within the drying chamber are all shown in the diagram above.

The heat equation in 2D is given by:

$$\frac{\partial T(x,y,t)}{\partial t} = \frac{k}{\rho c}\left(\frac{\partial^2 T(x,y,t)}{\partial x^2} + \frac{\partial^2 T(x,y,t)}{\partial y^2}\right)$$

In the heat equation above, k is the chamber's thermal conductivity in W/mK, c is the chamber's specific heat capacity in J/kgK, and d is the chamber's density in kg/m3.

III. RESULTS AND DISCUSSION

Temperature Measurement Results

The transient temperature distribution was determined in the following sections of the dryer: the glazing or cover (Tcov), the absorber (Tab), the intake (Tin), the two trays in the drying chamber; tray 1 (upper tray) (Tdcu) and tray 2 (lower tray) (Tdcd), the outlet (Tout), and the ambient temperature (Tam). The findings collected for each of the three days are shown in the tables below: The time is reported in 24-hour format and the temperatures are in degrees Celsius (0).

Table 4.1: Temperature data for day 1: 14th June, 2021

t(hrs)	Tab	Tdcu	Tdcd	Tout	Tin	Tcov	Tam
8.5	27.5	25.3	26.1	27.0	26.1	25.7	25.6
9.5	35.2	34.6	34.8	29.8	26.1	29.8	22.8
10.5	33.1	31.8	32.0	30.8	29.8	27.6	26.8
11.5	39.0	35.2	35.6	34.4	32.0	32.2	30.6
12.5	31.8	32.1	31.8	31.2	29.4	31.8	28.6
13.5	31.4	31.2	31.8	29.2	29.1	31.1	29.5
14.5	30.4	30.6	31.4	30.6	29.6	33.4	31.5
15.5	34.8	31.1	31.7	32.4	30.5	31.1	29.4
16.5	32.1	30.1	29.8	30.8	30.7	29.1	29.1

Published By:
International Journal of Engineering Research in Current Trends

Table 4.2: Temperature data for day 2: 15th June, 2021

t(hrs)	Tab	Tdcu	Tdcd	Tout	Tin	Tcov	Tam
9.5	28.8	31.4	30.4	28.7	27.7	29.1	26.6
10.5	40.1	35.6	36.4	38.6	38.0	30.1	27.1
11.5	38.8	39.1	38.3	40.1	36.2	35.6	30.6
12.5	43.0	37.1	36.9	37.8	39.1	38.2	33.1
13.5	33.1	28.3	30.1	33.5	31.6	24.6	21.8
14.5	29.3	28.6	28.1	28.0	26.9	24.4	23.1
15.5	30.1	27.9	27.8	28.3	27.8	26.8	26.1
16.5	30.8	24.1	24.3	30.7	28.1	21.8	21.6

Table 4.3: Temperature data for day 3: 16th June, 2021

t(hrs)	Tab	Tdcu	Tdcd	Tout	Tin	Tcov	Tam
9	31.1	30.4	30.3	30.4	31.1	29.9	28.1
10	29.1	28.7	28.8	28.4	28.5	29.1	28.1
11	28.8	26.9	26.7	26.8	26.4	26.8	26.0
12	30.4	27.5	27.5	27.1	26.9	26.8	26.3
13	43.1	38.8	38.4	32.3	31.7	29.1	27.1
14	33.6	31.6	32.7	25.1	24.1	30.2	26.0
15	33.9	32.4	32.1	25.7	23.4	31.5	25.7
16	34.6	32.8	32.6	23.9	21.6	30.3	25.5
17	31.8	27.8	27.6	24.6	22.7	31.3	24.6

Results of the Simulation

The temperature distribution in the drying chamber after (a) 30 seconds, (b) 60 seconds, (c) 90 seconds, and (d) 120 seconds is represented by the contour plots in Fig. (4.2). The temperature in the drying chamber rises progressively over time, as seen by the contour plots above. In the dryer, start with a temperature of To = 26. we set: T_{in} = 39.8, T_{fw} = 34.9, T_{bw} = 25, and T_{out} = 28.1 as boundary conditions. Heat flows from inlet and front wall to the outlet and back wall. The contour plots also reveal that the input temperature and front wall temperatures must be increased to achieve a temperature that can effect product drying in the drying chamber. Insolation has a direct impact on the front wall temperature, whereas solar collector performance has a direct impact on the inlet temperature.

This simplified model has shown that if the drying chamber material has a high thermal conductivity, low density, and low specific heat, temperature variations in the dryer can be improved. This accomplishment may be accomplished, for example, by utilising aluminium instead of silica glass, despite the fact that aluminium is significantly more expensive. However, because aluminium is opaque, utilising it throughout the house will damage the front wall insolation. The use of glass on the front wall is one approach to prevent poor insolation in the chamber.

Based on the above data, the following graphs were created:

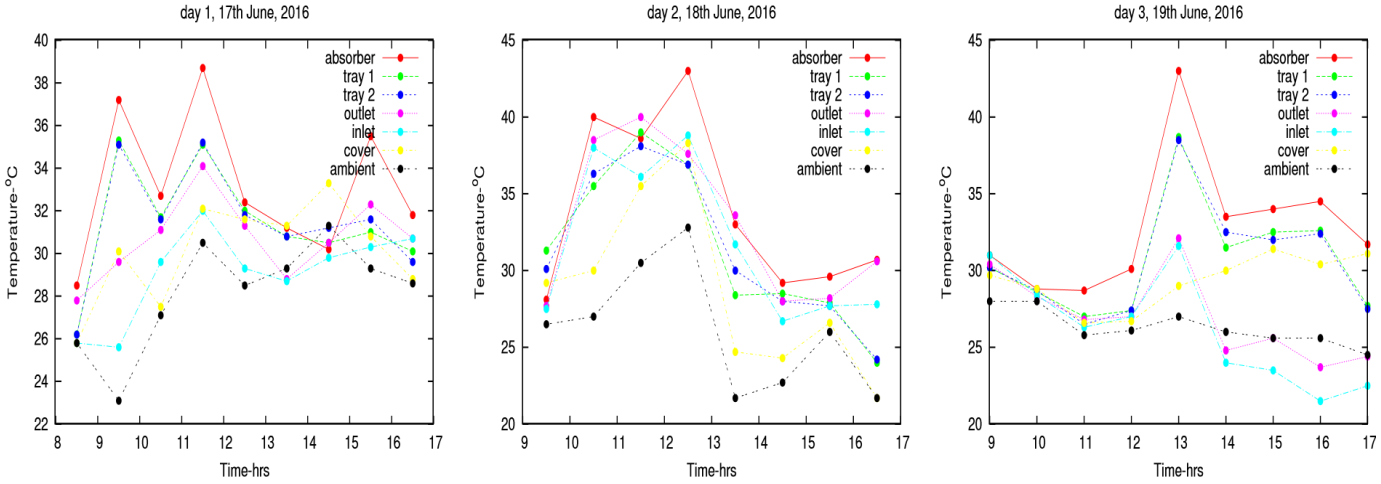

Figure 4.1: Transient temperature distribution in the major parts of the dryer

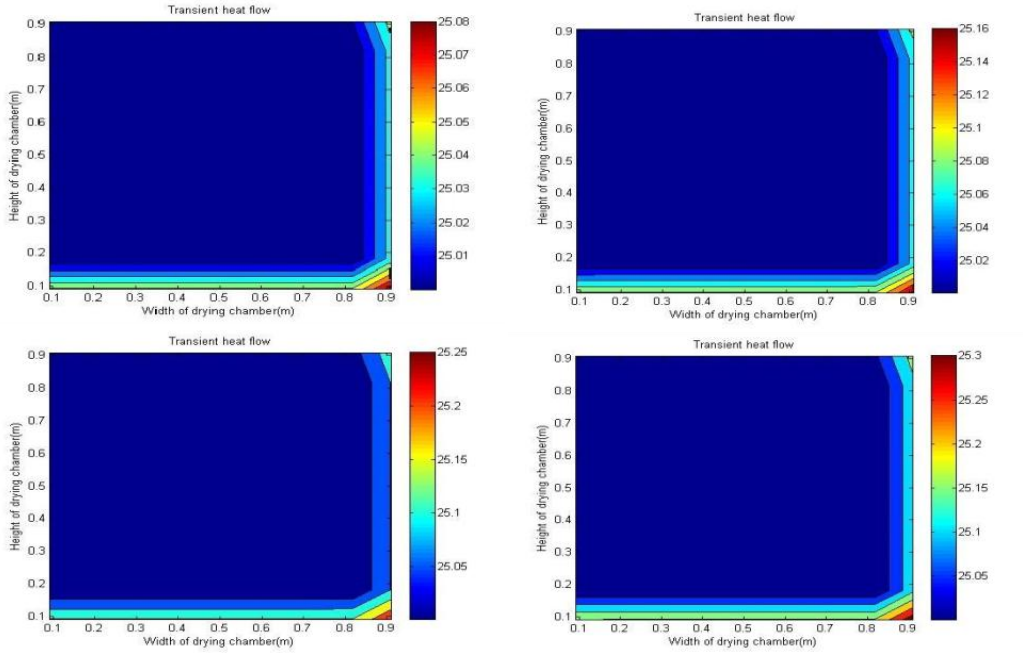

Figure 4.2: Contour plot of the temperature distribution in the dryer

To enable the temperature in the chamber to build up to the optimal level required for tomato drying, the drying should be allowed to run empty for a while before putting products into it.

Heat dispersion in larger dryers is slower than in smaller dryers with the same collector size. It's to be anticipated. Reduce the length and width of the dryer, for example, and the heat dispersion will improve.

Relative Humidity Measurement Results

Using the ARM approximation established in the previous chapter, the relative humidity in the ambient (rha) and drying chambers (rhu and rhd in the two trays) were calculated. The following information was gathered during each of the drying days. The relative humidity is expressed in percentages, while the time is expressed in 24-hour format.

Table 4.4: Relative humidity data for day 1: 14th June, 2021, dew point: 21

t(hrs)	Tdcu	Tdcd	Tam	Rhu	rhd	rha
8.50000000	26.3000009	26.2000008	26.1999992	72.8009217	72.8009217	75.1020204
9.50000000	35.2999994	35.1999985	22.9900004	43.5453255	44.1007905	88.1003979
10.500000	31.8000007	31.7000004	27.1000005	53.2618958	53.5645586	69.4270742
11.5000000	34.9999985	35.4000009	30.6000000	44.1367906	43.7942559	57.8253159
12.5000000	32.1000000	31.8999992	28.5100000	52.4654495	52.7611794	64.1147619
13.5000000	30.9999992	30.8999992	28.8999991	56.1570617	56.1170618	61.1119242
14.5000000	30.5000034	31.4000028	31.6999992	57.1253159	54.7947861	54.5842812
15.5000000	31.1000000	31.7000004	29.5999992	55.4218613	53.5645576	61.1009243
16.5000000	30.2000004	29.7000004	28.7000003	58.3458686	60.1001960	63.6148352

Published By:
International Journal of Engineering
Research in Current Trends

Table 4.5: Relative humidity data for day 2: 15th June, 2021, dew point: 20

t(hrs)	Tdcu	Tdcd	Tam	Rhu	rhd	rha
9.50000000	31.3999992	30.2000004	26.6000002	54.4842812	58.3458687	72.1100558
10.5000000	35.6000002	36.3999994	27.1000020	43.9757233	41.1240273	69.8353592
11.5000000	39.1200000	38.0999985	30.5000032	34.5092087	37.3783394	57.1253159
12.5000000	37.1000015	36.9000015	32.8999992	39.8943687	39.8943687	50.1571877
13.5000000	28.3999906	30.1000000	21.7100008	64.3571335	58.6813828	95.8011246
14.5000000	28.6000000	28.1000000	22.8000009	63.9847618	65.6711943	90.2420364
15.5000000	27.9999996	27.8000009	26.0000000	66.1559830	67.2331436	74.1706345
16.5000000	24.0000000	24.2220008	21.7000008	83.3387833	82.3442917	95.8011246

Table 4.6: Relative humidity data for day 3: 16th June, 2021, dew point: 20

t(hrs)	Tdcu	Tdcd	Tam	Rhu	rhd	rha
9.00000000	30.4000008	30.5000008	28.0000000	54.5486351	54.5486351	61.8372612
10.0000000	28.6000004	28.9000008	28.0000000	59.7158585	59.3703232	61.8372612
11.0000000	27.2000000	26.6000000	25.7999992	65.5643158	67.6222549	70.4749390
12.0000000	27.4999996	27.5999996	26.1000004	64.1439529	64.0439529	69.1360626
13.0000000	38.6000008	38.6000000	27.0000000	32.8296188	34.2980652	65.7643158
14.0000000	31.5000000	32.5000000	26.1430000	50.6331044	47.8700081	69.5562723
15.0000000	32.5240000	32.4000000	25.6000084	47.7700081	49.3393280	71.4147141
16.0000000	32.5999985	32.6000015	25.6000004	47.5013657	47.9424015	71.3147141
17.0000000	28.1000008	27.5000000	24.5000000	62.9297104	63.8700821	76.0400009

The following graphs were plotted based on the above data:

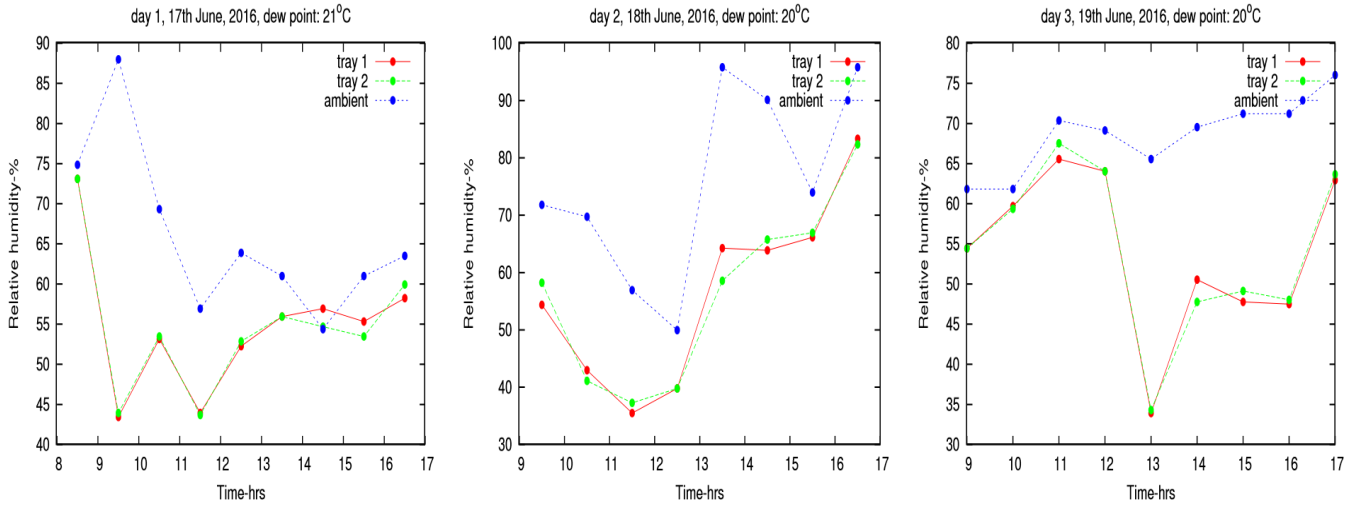

Figure 4.3: Transient relative humidity distribution in the major parts of the dryer

Mass Loss/Moisture Content

The loss in mass or mass loss *ml* of the tomatoes were calculated during the drying hours with the formula:

$$ml = m_i - m_f$$

where ml represents mass loss, mi represents starting mass, and mf represents final mass. The product is initially weighed with a weighing balance to ascertain its initial mass mi at a specific moment in order to compute the loss in mass during a given time interval. The product is weighed again after the time interval to calculate the final mass mf. Observation reveals that mf mi, indicating that drying occurs.

The percentage moisture content %*MC* is calculated based on the following formula:

$$MC = \frac{m_i}{m_f} - 1 \times \frac{100}{1}$$
$$= \frac{ml}{m_f} \times \frac{100}{1}$$

where %*MC* = percentage moisture content, m_i = initial mass, and m_f = final mass.

Table 4.7: Decrease in product's mass as a function of time

t(hrs)	0	4	5	8	18	19	20	21	22	24	41	43	44
m(kg)	1.00	0.95	0.85	0.75	0.50	0.46	0.35	0.32	0.30	0.24	0.22	0.21	0.21

When the change in the product's mass is insignificant and the appropriate colour is reached, the mass of the product is lowered from its initial value of 1.00kg to a final value of 0.21kg, as shown in Table(4.7). Over-drying occurs after this value is exceeded, resulting in excessive drying and wrinkling of the items.

Kinetics of Drying

Drying kinetics is the study of how quickly products dry under different environments. Three basic drying models for tomatoes are commonly used to determine the drying rate constant of tomatoes [22, 24]:

1. Henderson and Pabis (1974) : $MR = exp(-kt^n)$, where k =drying rate constant, n = drying coefficient, $1 \leq n \leq 2$
   In this model, effects of temperature and time on the rate of drying were considered.
2. Newton(1985) : $MR = exp(-kt)$, where k = drying rate constant, MR = moisture ratio, t = time This is a special case of the Henderson and Pabis model (when $n = 1$).
3. Midilli et al(2002): $MR = aexp(-k^n t) + bt$, k,b = drying rate constants, a,n = drying coefficients, $1 \leq n \leq 2$, $a \leq 1$
   This model studied effects of temperature, relative humidity, dew point, and time on the rate of drying.

$$MR = \frac{M}{M_o}, M_o = \text{initial moisture content of the product,}$$

M = moisture content of the product at any time. By fitting our experimental data on

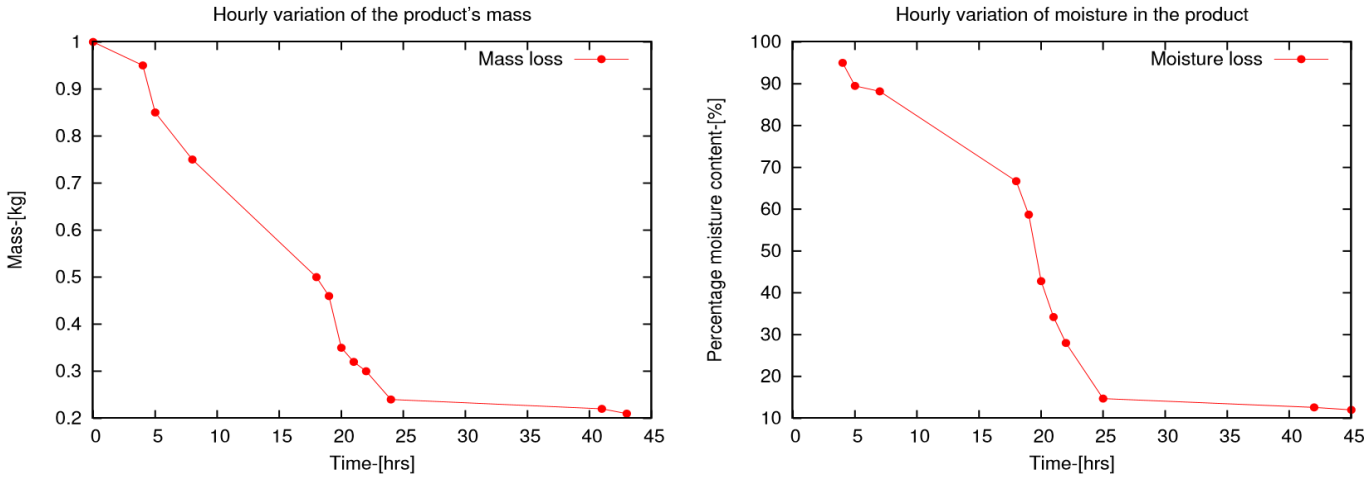

Figure 4.4: Drying results the drying models using the least-squares regression method, the following results were obtained; the Newton model gave the best fit.

Published By:
International Journal of Engineering
Research in Current Trends

Henderson and Pabis*:* k = 0.25units/h = 6.00units/day, n = 1.44

Newton: k = 0.12units/h = 2.88units/day

Midilli et al: k = 0.32units/h = 7.68units/day, a = 1.01, n=1.43, b = 0.0135units/h = 0.324units/day

Analysis of Results

The ideal temperature range for drying tomatoes in a drying chamber is 40°C to 80°C [24]. The temperature in the drying chamber reached a maximum of 35oC at 9: 30am on day 1, a maximum of 38.8oC at 11: 30am on day 2, and a maximum of 43.0oC at 01:00pm on day 3, according to our results in Tables (4.1, 4.2, and 4.3) and Fig. (4.1). These figures illustrate that time and weather conditions have an impact on insolation and dryer performance. Day 1 was rainy with low insolation, however days 2 and 3 were sunny with high insolation after sunrise. As a result, on days 2 and 3, the drying chamber temperature is comparable to the recommended drying chamber temperature range.

The relative humidity of a drying chamber is the moisture content of the air within it at any particular time. It is dependent on the temperature and dew point. The ideal relative humidity range for tomato drying in a drying chamber is 20% to 60% [24]. The relative humidity in the drying chamber achieved a minimum value of 43.54 percent at 9: 30 a.m. on day 1, a minimum of 34.5 percent at 11: 30 a.m. on day 2, and a minimum of 32.8 percent at 1: 00 p.m. on day 3, according to our data in Tables (4.4, 4.5, and 4.6) and Fig. (4.3). As a result, on day 1, day 2, and day 3, the drying chamber relative humidity falls within the optimal drying chamber relative humidity range. The drier can reduce the moisture content of 1kg of tomatoes from 96 percent to 13 percent in 45 hours, as shown in Fig. (4.4). The dryer has a capacity of 1kg of items per tray.

While the relative humidity in the drier was suitable for tomato drying, the temperature in the drying chamber did not reach to the recommended limit. Poor insolation on the specified drying days, heat losses through the glass walls and roof, and excessive relative humidity in the ambient are all probable causes.

IV. CONCLUSION

Throughout the trial, the temperature of the drying chamber stayed higher than the ambient temperature, while the relative humidity in the ambient temperature remained high. During the active drying hours, the drying chamber reached a maximum temperature of 39.12^{o}C and a minimum relative humidity of 33.9 percent, which is ideal for drying tomatoes. Within 45 hours of drying time, the drier can reduce the moisture content of 1kg of tomatoes from 96% to 13%. The dryer has a capacity of 1kg of items per tray.According to our drying experiment, tomatoes can be dried for three or more days during the rainy season before reaching equilibrium.

REFERENCES

[1] A, Sharma et. al (2009) Solar-energy drying systems: a review, Renewable and sustainable energy review, 13(67): 1185-1210.

[2] D.R. Pangavhane et. al (2003) Design, Development and performance testing of a new natural convection solar dryer, Energy 27(6):579-590.

[3] M. A. Karim and M.N.A. Hawlader (2004) Development of Solar air Collectors for drying Applications, Energy conversion and Management, 45(3): 329-344.

[4] E.K. Akpinar and F. Kocyigit (2010) Energy and exergy analysis of a new flat plate solar air heater having different obstacles on absorber plates. Applied energy. 87(11): 3438-3450.

[5] A.O Akinola (1999)Development and performance evaluation of a mixed-mode solar food dryer. M. Eng. Thesis, Federal University of Technology, Akure, Nigeria.

[6] Bal, L. M et. al (2010) Solar dryer with thermal energy storage for drying Agricultural food products: A review. Renewable and Sustainable Energy Reviews, 14 (8): 2298-2314

[7] Blair R. et. al (2007)Design of a solar-powered fruit and vegetables dryers.

[8] Abdulelah All Al-Jumaah, Abdullah Mohamed Aslri (2010)Design and construction of a solar drying system for food preservation

[9] Bennamoum,L,Belhamri(2003 A design and simulation of a solar dryer for agricultural products. Journal of Food Engineering, 59:259-266.

[10] M.A. EL-Shiatry et. al (2002) Drying fruits and vegetables with solar energy in Egypt. AMA. 4:61-64.

[11] Majumdar, A.S and Law, C.L (2010) Drying technology: Trends and applications in post-harvest processing. Food and Bioprocess Technology. 3(6): 843-852.

[12] Bolaji, B.O and Olalusi A.P (2008) Performance evaluation of a mixed mode solar dryer, Journal of Technology, A publication of Assumption University, Bangkok Thailand 11(4): 225-231

[13] Bolaji, B.O (2005) Performance evaluation of a simple solar dryer for food preservation. In proceeding of the 6th Annual Engineering Conference of School Engineering and Technology, Federal University of Technology, Minna, Nigeria.

[14] Abdulelah All Al- Jumaah and Abdullah Mohamed Aslri (2010) Design and construction of a solar drying system for food preservation.

[15] Ion, I.V and Martins, G.J (2006) Development and testing of a solar air collector glass, University of Minho.